Coexpression of α and β Subunits of the Rod Cyclic GMP-Gated Channel Restores Native Sensitivity to Cyclic AMP: Role of D604/N1201

Frédérique Pagès, Michèle Ildefonse, Michel Ragno, Serge Crouzy, and Nelly Bennett
Laboratoire de Biophysique Moléculaire et Cellulaire (URA CNRS 520), DBMS, C.E.A.-Grenoble, Grenoble, France

ABSTRACT Coexpression of the βwt and αwt subunits of the bovine rod channel restores two characteristics of the native channels: higher sensitivity to cAMP and potentiation of cGMP-induced currents by low cAMP concentrations. To test whether the increased sensitivity to cAMP is due to the uncharged nature of the asparagine residue (N1201) situated in place of aspartate D604 in the β subunit as previously suggested (Varnum et al., 1995, *Neuron.* 15:619–625), we compared currents from wild-type (αwt and $\alpha wt/\beta wt$) and from mutated channels (αD604N, αD604N/βwt, and $\alpha wt/\beta$N1201D). The results show that the sensitivity to cAMP and cAMP potentiation is partly but not entirely determined by the charge of residue 1201 in the β subunit. The D604N mutation in the α subunit and, to a lesser extent, coexpression of the βwt subunit with the αwt subunit reduce the open probability for cGMP compared to that of the αwt channel. Interpretation of the data with the MWC allosteric model (model of Monod, Wyman, Changeux; Monod et al., 1965, *J. Mol. Biol.* 12:88–118) suggests that the D604N mutation in the α subunits and coassembly of α and β subunits alter the free energy of gating by cAMP more than that of cAMP binding.

INTRODUCTION

The cGMP-gated channels of retinal rods are responsible for light-induced hyperpolarization of the photoreceptor cell: hydrolysis of cGMP upon activation of the light-sensitive cascade of phototransduction leads to closure of the channels and reduction of the cationic current that enters the cell in the dark. Cyclic nucleotide-gated (CNG) channels are directly activated by binding of cyclic nucleotide to a site situated in the cytoplasmic C-terminal region. This site was identified by its high sequence homology with other known cyclic-nucleotide binding proteins: the CRP protein of *Escherichia coli* and regulatory subunits of the cGMP- and cAMP-activated protein kinases (Kaupp et al., 1989; Shabb and Corbin, 1992). Within this site, a residue, situated near the end of the αC helix of the binding site in the rod α subunit (D604), was shown to play an important role in nucleotide specificity: substitution of the charged aspartate residue by uncharged glutamine or asparagine in the rod channel modifies the agonist specificity, and substitution by the non polar methionine residue inverts the specificity, which becomes cAMP > cIMP > cGMP (Varnum et al., 1995). Both the rod and olfactory native channels are heterooligomeric proteins, composed of at least two types of subunits: α (CNG1) and β (CNG4) for the rod channel (Chen et al., 1993; Körschen et al., 1995; Biel et al., 1996), and subunit 1 (CNG2), subunit 2 (CNG5), and a recently discovered CNG4.3 subunit related to the rod β subunit for the olfactory channel (Liman and Buck, 1994; Bradley et al., 1994; Sautter et al., 1998). For the olfactory channel, coexpression of subunit 2 (Liman and Buck, 1994; Bradley et al., 1994) or of CNG4.3 with subunit 1 was found to increase the sensitivity to cAMP, whereas coexpression of the three subunits almost restores native sensitivity (Sautter et al., 1998). Fodor and Zagotta (1996), Gordon et al. (1996), and Shammat and Gordon (1999) also report an increased ratio of cAMP-induced to cGMP-induced currents when the human rod β subunit is coexpressed with the bovine rod α subunit. In the rod β subunit, as in the olfactory subunit 2 and in CNG4.3, the residue corresponding to the acid residue D604 in the rod α subunit (or E581 in the olfactory subunit 1) is an uncharged residue (M in the rat olfactory subunit 2, N in CNG4.3 and in the rod β subunit). Fodor and Zagotta (1996) proposed that the β subunit may be responsible for the increased sensitivity of the native rod channel compared to the expressed α subunit and suggested that the uncharged residue at the position equivalent to D604 (N1201) might explain this effect.

Another characteristic of native rod channels is potentiation of cGMP-induced currents by low concentrations of cAMP (Furman and Tanaka, 1989; Ildefonse et al., 1992); a communication concerning the study of this phenomenon on expressed heteromeric channels has been published (Scott and Tanaka, 1998), but it is not known whether it could be related to a higher sensitivity of the β subunits to cAMP.

We report here a comparative study of the sensitivity to cGMP and cAMP and of cAMP potentiation of cGMP-induced currents of expressed channels consisting of bovine α subunits or of coexpressed bovine α and β subunits. The role of the residue in position 604 in the α subunit and in the corresponding position in the β subunit (1201) is studied by comparing currents from wild-type channels (αwt and $\alpha wt/\beta wt$) and from mutated channels (αD604N, αD604N/βwt, and $\alpha wt/\beta$N1201D).

Received for publication 16 May 1999 and in final form 7 December 1999.

Address reprint requests to Dr. Nelly Bennett, BMC/DBMS, CEA-Grenoble, 17 rue des Martyrs, 38054 Grenoble cedex 9, France. Tel.: 33-4-76-88-48-49; Fax: 33-4-76-88-54-87; E-mail: nelly.bennett@cea.fr.

0006-3495/00/03/1227/13 $2.00

MATERIALS AND METHODS

Channel expression

The bovine α subunit cDNA (Kaupp et al., 1989) was a gift of Prof. U. B. Kaupp. The β subunit cDNA was amplified by polymerase chain reaction

from bovine retinal cDNA, using oligonucleotide primers chosen according to the published sequence (Körschen et al., 1995). Retinal mRNA was prepared from fresh retinas with the Dynabeads mRNA DIRECT kit (DYNAL), and cDNA was synthesized using the First-strand cDNA synthesis kit (Amersham Pharmacia Biotech). The N-terminal domain, which was shown to have no effect on the sensitivity to nucleotides (Körschen et al., 1995), was deleted up to G571, and a methionine residue was introduced before V572 for translation initiation. A Kozak consensus sequence was engineered upstream of the ATG codon, and the truncated cDNA was inserted in the high expression vector pGemHe downstream of the untranslated sequence of the *Xenopus* β-globin gene (Liman et al., 1992). The cDNA sequence of our β subunit from the codon corresponding to V572 is 100% identical to that of CNG4c (Biel et al., 1996), leading to several modifications compared to the sequence published by Körschen et al. (1995): S/A substitution at position 1283, R/A at position 1289, D/E at position 1336, and insertion of A between D1336 and A1337 (all amino acid numbers refer to the sequence of Körschen et al.). Mutations (αD604N and βN1201D) were created by replacing the GAT (aspartate 604) codon with AAT (asparagine) in the α cDNA, and the AAC (asparagine 1201) codon with GAC (aspartate) in the β cDNA. Mutated sequences were verified by sequencing.

Capped mRNAs were synthesized in vitro from linearized plasmids in the presence of RNA cap structure analogs (New England Biolabs) and injected into *Xenopus* oocytes (25 ng/oocyte for macroscopic currents or 0.25 ng/oocyte for single channels). For coexpression of α and β subunits, β mRNA and α mRNA were mixed and injected into the oocyte. To reduce the probability of forming homomeric α channels, the β:α mRNA ratio was 2 for all experiments (except for single-channel analysis, where it was 3). Different ratios were not tested. Oocytes were incubated for 4–10 days in Barth's medium before measurements. As previously reported (Chen et al., 1993; Körschen et al., 1995), the wild-type β subunit did not form functional channels when expressed alone.

Patch-clamp recording of excised inside-out patches

The solution in the pipette and in the perfusion medium was 100 mM KCl, 10 mM EGTA/KOH, 10 mM HEPES/KOH (pH 7.2). The cytoplasmic face of the patch was superfused by solutions containing variable nucleotide concentrations, using a RSC100 rapid solution changer (Bio-Logic, Claix, France). Currents induced by voltage steps (500 ms, $\pm$80 mV) were recorded with a RK-400 patch amplifier (Bio-Logic), low-pass filtered at 300 Hz, and digitized at 1 kHz (macroscopic currents, each record averaged three times), or at 10 kHz and digitized at 33 kHz (single channels), using pCLAMP 6.0 (Axon Instruments). For macroscopic currents, the series resistance was compensated for (resulting value < 1 MΩ). Dose-response curves were obtained by plotting the current at +80 mV as a function of nucleotide concentration after subtraction of the leak current.

Probability of channel opening

$P_{0\max(cGMP)}$ (open probability at saturation of cGMP) was estimated by two methods:

1. From the ratio of currents at saturation of cGMP in the absence and in the presence of Ni^{2+} (1 μM). Micromolar concentrations of cytoplasmic Ni^{2+} were previously shown to potentiate cGMP-induced currents (Ildefonse et al., 1992; Gordon and Zagotta, 1995), and the $I_{\max(cGMP)}/I_{\max(cGMP + Ni)}$ ratio was shown to be very close to the $P_{0\max(cGMP)}$ value obtained from single-channel measurements for homomeric α (wild type and mutated) channels (Sunderman and Zagotta, 1999). The cGMP-induced currents were measured several times (before and after addition of Ni^{2+}) until stabilization; the effect of Ni^{2+} was at maximum after 4–5 min. For these experiments, high-grade KCl or NaCl (containing less than 0.025 ppm transition metals; Merck) was used, and the HEPES concentration was reduced to 5 mM. No EGTA or EDTA was added to the perfusion medium; the solution in the pipette contained 200 μM EDTA and 500 μM niflumic acid.

2. From single-channel records analysis: Amplitude histograms were computed from single-channel records at +80 mV (record duration: 16–38 s for αwt, 10–50 s for $\alpha wt/\beta wt$, 18–77 s for αD604N), using Bio-Patch software (Bio-Logic). Records were sampled at 33 kHz and numerically filtered (Hanning window) at 4 and 1 kHz. The histograms were fitted with two or three Gaussian curves.

Curve fitting

Fits of dose-response curves were calculated with Microcal Origin software. The error on the value of the parameters calculated by the program is $\text{error}(i) = \sqrt{(C(i)(i)\cdot\chi^2)}$, where $C(i)(i)$ is the covariance matrix for n parameters ($i = 1, n$).

Hill equation

$I/I_{\max} = 1/(1 + (EC_{50}/X)^{nH})$, where EC_{50} is the ligand concentration that gives the half-maximum effect, n_H is the Hill number, and X is the ligand concentration.

Monod-Wyman-Changeux model

Assuming that the rod channel is a tetramer (Liu et al., 1996), the proportion of channels in the R (open) state is given by $\bar{R} = (1 + X/K_R)^4/((1 + X/K_R)^4 + L\,(1 + cX/K_R)^4)$, in which X is the ligand concentration, $L = [T]/[R]$, T corresponds to the closed state, and $c = K_R/K_T$ (dissociation constants of the ligand for the R and T states). Predictions of this model are, briefly, as follows:

1. The EC_{50} depends on K_R, c, and L.
2. $\bar{R}_{\max}$ depends on c and L.
3. L is independent of the ligand but is a characteristic of the protein; it can therefore depend on the subunit composition of the channel (α alone or $\alpha + \beta$) and can be modified by a mutation. Modifying L is expected to shift the dose-response curves for different ligands (for example, cGMP and cAMP) and to modify the value of $\bar{R}$ at saturation of the different ligands ($\bar{R}_{\max}$) in the same direction.
4. The parameter c, on the other hand, depends on both the protein (therefore on the subunit composition and on the presence of mutations) and the ligand; for a given value of L, $\bar{R}_{\max}$ only depends on the value of c for this ligand (increasing c reduces $\bar{R}_{\max}$).
5. Spontaneous openings are determined by L, whereas ligand-induced openings are determined by $L^*(c)^n$.

Statistics

The significance of the difference between two populations of data was analyzed by independent t-tests using Origin software.

Chemicals

L-*cis*-Diltiazem was a gift of Synthelabo Recherche (Bagneux, France).

RESULTS

Coexpression of the βwt subunit with the αwt subunit increases the sensitivity to cAMP; role of residues D604 in α subunit and N1201 in β subunit

Plots of currents at saturating cGMP and cAMP concentrations obtained from the same patch in one experiment with

homomeric αwt channels and in one experiment with heteromeric channels expressed in oocytes coinjected with the αwt and βwt subunit mRNAs are shown in Fig. 1 *A*. The presence of the β subunit clearly increases the current at saturating cAMP concentration compared to the current at saturating cGMP concentration. The effect is observed independently of the voltage but is more evident at positive voltage because of the larger amplitude of cAMP-induced currents. To test whether the increased sensitivity conferred by coexpression of the β subunit is due to the uncharged residue N1201, as suggested by the results of Varnum et al. (1995) and Fodor and Zagotta (1996), we constructed a mutated α subunit in which D604 is replaced by the neutral asparagine residue present in the β subunit at the corresponding place (αD604N) and the symmetric mutated β subunit N1201D.

Mean $I_{max(cAMP)}/I_{max(cGMP)}$ ratios at +80 mV and −80 mV from several experiments with different channel compositions are plotted in Fig. 1 *B*, and values are listed in Table 1. Coexpression of the βwt subunit with the αwt subunit increases the $I_{max(cAMP)}/I_{max(cGMP)}$ ratio, although to a lesser extent than does the D604N mutation in the α subunit, which is as expected if the effect is due to the uncharged N1201 or N604 residues. However, upon coexpression of the mutated βN1201D subunit with the αwt subunit, the $I_{max(cAMP)}/I_{max(cGMP)}$ ratio remains intermediate between those of the αwt and $\alpha wt/\beta wt$ channels, and coexpression of βwt with αD604N further increases the $I_{max(cAMP)}/I_{max(cGMP)}$ ratio compared to αD604N channels. These effects are more clearly observed at positive voltage.

Dose-response curves at +80 mV for each channel composition are shown in Fig. 2. The values of EC_{50} and n_H for cGMP and cAMP indicated in Table 1 are the parameters of the fits to the Hill equation of all of the data (normalized to the current at saturation of nucleotide) from all experiments. Inversely to the variation of the $I_{max(cAMP)}/I_{max(cGMP)}$ ratio, the EC_{50} for cAMP varies in the order $\alpha wt > \alpha wt/\beta$N121D $> \alpha wt/\beta wt > \alpha$D604N $> \alpha$D604N/βwt. The errors calculated by the program suggest that the EC_{50} for cAMP of the five channel types are significantly different, although this assumption should be made with caution because of the large variations between experiments. The larger effect is observed upon coexpression of βwt with αD604N, compared to all other channel types. The population of EC_{50} obtained from the fit of each experiment for αD604N/βwt channels is also significantly different from that of all other channel types, including αD604N ($p < 10^{-2}$); therefore, coassembly of the βwt subunit with αD604N seems to further reduce the EC_{50} for cAMP compared to αD604N channels, suggesting that the effect is not only due to the charge of residues N1201 or N604.

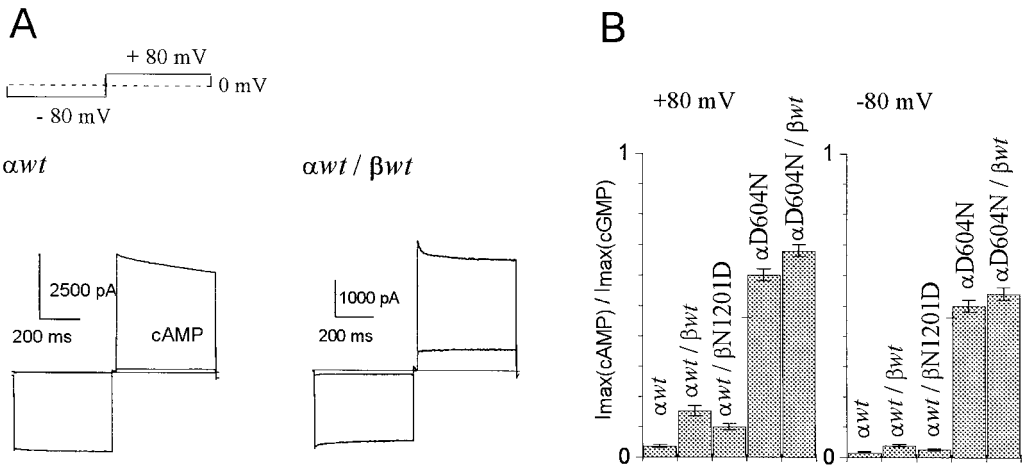

FIGURE 1 Comparison of cGMP- and cAMP-induced currents for different channel compositions. (*A*) Examples of current recordings at saturating cGMP (0.5 mM) and cAMP (20 mM) concentrations from oocytes injected with αwt or $\alpha wt + \beta wt$ mRNAs. The voltage step protocol is shown above. When accumulation/depletion was observed, the value for the current was taken as the average between the initial value and the value at 500 ms; this approximation gives values close to those obtained with the correction proposed by Zimmerman et al. (1988). (*B*) Mean ratios of the current at saturation of cAMP and cGMP for different channel compositions. Saturating concentrations were 20 mM for cAMP and 0.5 mM (αwt, $\alpha wt + \beta wt$, $\alpha wt + \beta$N1201) or 5 mM (αD604N, αD604N + βwt) for cGMP. For each patch, cAMP- and cGMP-induced currents were measured several times, as closely as possible, with control measurement of the leak current before and after. Mean values of $I_{max(cAMP)}/I_{max(cGMP)}$ (± SE) at +80 mV and −80 mV are listed in Table 1. $I_{max(cGMP)}$ was between 1098 pA and 4953 pA (mean value ± SE:2733 pA ± 378 pA) at + 80 mV and between 2474 and 5127 (mean value 4009 pA ± 371 pA) at −80 mV for αwt; between 1188 pA and 3969 pA (mean value ± SE: 2505 pA ± 242 pA) at +80 mV and between 1440 pA and 4778 pA (mean value ± SE: 2968 pA ± 373 pA) at −80 mV for $\alpha wt + \beta wt$; between 660 pA and 3500 pA (mean value ± SE: 2425 pA ± 300 pA) at +80 mV and between 2032 pA and 4749 pA (mean value ± SE: 3102 pA ± 277 pA) at −80 mV for $\alpha wt + \beta$N1201D; between 455 pA and 3653 pA (mean value ± SE: 1733 pA ± 272 pA) at + 80 mV and between 132 pA and 2200 pA (mean value ± SE: 938 pA ± 168 pA) at −80 mV for αD604N; between 431 pA and 2623 pA (mean value ± SE: 1353 pA ± 184 pA) at + 80 mV and between 124 pA and 2200 pA (mean value ± SE: 713 pA ± 131 pA) at - 80 mV for αD604N + βwt.

TABLE 1 $I_{max(cAMP)}/I_{max(cGMP)}$ ratios and Hill parameters of cGMP and cAMP dose-response curves for different subunit compositions

	$I_{max(cAMP)}/I_{max(cGMP)}$		cGMP		cAMP	
mRNA injected	+80 mV	−80 mV	EC_{50} (μM)	n_H	EC_{50} (μM)	n_H
αwt	0.036 ± 0.005 (15)	0.016 ± 0.002 (8)	29.9 ± 0.8 (8)	2.2 ± 0.2 (8)	2077 ± 172 (8)	1.32 ± 0.12 (8)
$\alpha wt + \beta wt$	0.153 ± 0.016 (11)	0.039 ± 0.004 (10)	35 ± 0.6 (11)	2 ± 0.1 (11)	1607 ± 31 (9)	1.45 ± 0.04 (9)
$\alpha wt + \beta$N1201D	0.10 ± 0.01 (12)	0.026 ± 0.003 (12)	29.8 ± 0.4 (11)	2.2 ± 0.1 (11)	1858 ± 33 (11)	1.55 ± 0.04 (11)
αD604N	0.60 ± 0.02 (15)	0.5 ± 0.02 (19)	468 ± 21 (7)	1.6 ± 0.1 (7)	1527 ± 75 (8)	1.4 ± 0.1 (8)
αD604N + βwt	0.68 ± 0.02 (15)	0.54 ± 0.02 (19)	345 ± 7 (7)	1.5 ± 0.1 (7)	923 ± 25 (6)	1.6 ± 0.1 (6)

The $I_{max(cAMP)}/I_{max(cGMP)}$ ratios (from Fig. 1) measured for αwt and $\alpha wt + \beta wt$ are significantly different with $p < 5 \times 10^{-8}$ (+80 mV) and $p < 0.001$ (−80 mV); those for αwt and $\alpha wt + \beta$N1201 with $p < 5 \times 10^{-8}$ (+80 mV) and $p < 0.01$ (−80 mV); and those for $\alpha wt + \beta wt$ and $\alpha wt + \beta$N1201 with $p < 5 \times 10^{-8}$ (+80 mV) and $p < 0.01$ (−80 mV). For αD604N and αD604N + βwt, the $I_{max(cAMP)}/I_{max(cGMP)}$ ratios are significantly different at +80 mV with $p < 0.01$, but the difference is less significant at −80 mV ($p = 0.08$). EC_{50} and n_H were obtained from the fit to the Hill equation (shown in Fig. 2) of all data points from several experiments (normalized to the current at saturating cGMP or cAMP concentrations). The errors in the values of the parameters are calculated with Origin software when fitting with all points (see Materials and Methods). The means of the values of EC_{50} obtained from fitting individual experiments are close to the values indicated in the table. SEM are between 1.3 and 3 times larger than the error in fitting all of the points. The number of experiments (i.e., for dose-response curves, the number of data points for each nucleotide concentration) is indicated in parentheses.

Note also that whereas a 15-fold increase of EC_{50} for cGMP is observed for αD604N channels compared to αwt channels, only a limited (if significant) increase is observed when βwt is coexpressed with αwt.

Estimates for the open probability of homomeric (αwt, αD604N) and heteromeric (αwt/βwt) channels

The $P_{0max(cGMP)}$ of αwt, $\alpha wt/\beta wt$, and αD604N channels was estimated by two different methods (see Materials and Methods): from the $I_{max(cGMP)}/I_{max(cGMP+Ni}$ ratio (Gordon and Zagotta, 1995; Varnum et al., 1995; Varnum and Zagotta, 1996; Sunderman and Zagotta, 1999) and from single-channel recordings (Fig. 3). Values obtained with the two methods are indicated in Table 2. They are similar for αwt and $\alpha wt/\beta wt$ channels, but the agreement is less satisfying for αD604N channels (see below). Nevertheless, whatever the method used, $P_{0max(cGMP)}$ decreases in the order $P_{0max(cGMP)}$ (αwt) > $P_{0max(cGMP)}$ ($\alpha wt/\beta wt$) > $P_{0max(cGMP)}$ (αD604N). $P_{0max(cAMP)}$ can be deduced from the value of $P_{0max(cGMP)}$ and the $I_{max(cAMP)}/I_{max(cGMP)}$ ratio (Table 1) and varies in the inverse order $P_{0max(cAMP)}$ (αwt) < $P_{0max(cAMP)}$ ($\alpha wt/\beta wt$) < $P_{0max(cAMP)}$ (αD604N).

When αwt and βwt mRNAs were coinjected, the nature of the expressed single channel was checked by the addition of 50 μM L-*cis*-diltiazem (Fig. 3, *a* and *b*); for 12 of 13 records, diltiazem reduced P_0 to almost 0, whereas it was only reduced by less than 20% for the other, as well as for patches from oocytes injected with α mRNA only (9–18%, four patches). This suggests that the population of channels is mainly composed of heteromeric channels when the two mRNAs are coinjected, consistent with the results of Shammat and Gordon (1999), who suggest that channel assembly may be biased toward the inclusion of β subunits. In our experiments, the unitary current was similar for all single $\alpha wt/\beta wt$ channel records (1.38 ± 0.05 pA at +80 mV, nine patches), suggesting that the population of heteromeric channels is also homogeneous, in contrast to the results of Torre et al. (1997), who describe three distinct heteromeric channel types. The unitary current is also similar to that of αwt channels (1.35 ± 0.04 pA, four patches) and αD604N channels (1.37 ± 0.07 pA, nine patches). The low value compared to published data can be related to the fact that the channel conductance is smaller when the permeating cation is K^+ than when it is Na^+ (Nizzari et al., 1993; G_{Na}/G_K = 1.24 at +140 mV).

As the $P_{0max(cGMP)}$ for αD604N channels measured with the Ni^{2+} method (0.35 ± 0.04, Table 2) was considerably higher than that measured by Sunderman and Zagotta (1999) (0.08 with the same method), we asked whether this could be related to the nature of the permeating ion (which is K^+ instead of Na^+ in our experiments); when K^+ was replaced by Na^+, $P_{0max(cGMP)}$ was indeed reduced to 0.20 ± 0.03 (eight patches), still remaining higher, however, than the value reported by Sunderman and Zagotta (1999). In our experiments, the onset of the cGMP-induced current is slow, reaching a steady state in 1–2 min, and single-channel records of αD604N channels reveal a heterogeneity in the channel activity that was not previously reported. The $P_{0max(cGMP)}$ value obtained from single-channel analysis for αD604N channels varies with time for a given patch, usually starting with a low value (0.08 ± 0.03, six different patches) within the first minute in the presence of cGMP, and then increasing to higher values (0.41 ± 0.09, eight patches), as in the example shown in Fig. 3 *c*. The maximum $P_{0max(cGMP)}$ value obtained was also variable for different patches (between 0.15 and 0.83, eight patches). For three of these patches, long records (4–6 min) were analyzed, showing that after reaching a higher value, the activity did not clearly stabilize, but varied with periods of tens of seconds at any level between the two extreme values, and with long closed periods of several seconds or tens of seconds. The mean value indicated in Table 2 (0.25 ± 0.04) includes all

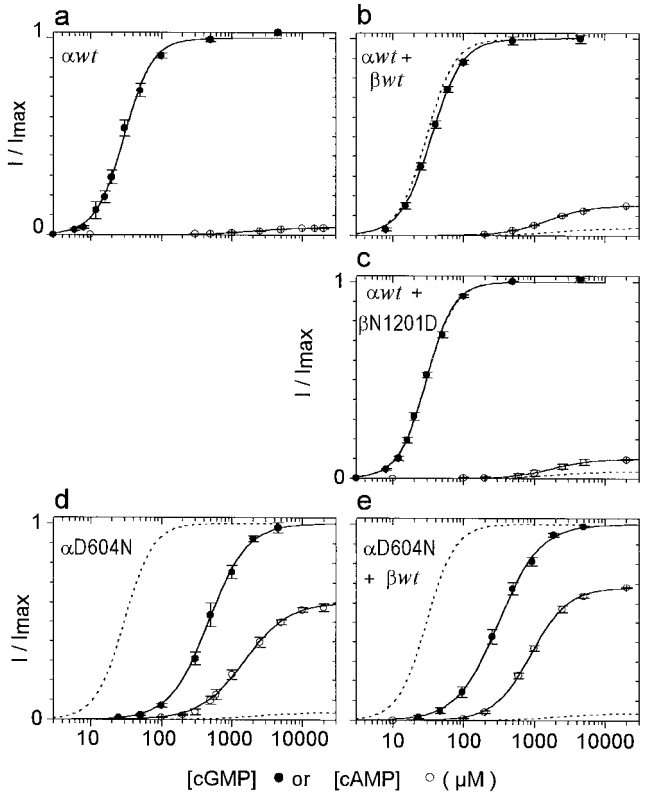

FIGURE 2 Dose-response curves for cGMP- and cAMP-induced currents from oocytes injected with mRNAs for *αwt* (*a*), *αwt* + *βwt* (*b*), *αwt* + *β*N1201D (*c*), *α*D604N (*d*), and *α*D604N + *βwt* (*e*). ●, cGMP; ○, cAMP. Several dose-response curves for cGMP and cAMP were measured for each channel composition (different patch for each experiment). For each experiment, currents were normalized to the current at saturating cGMP or cAMP concentration (calculated from the fit of the raw data to the Hill equation). Hill fits shown on the graphs were obtained using all of the normalized data points from all experiments for each channel composition. The cAMP dose-response curves were then multiplied by the $I_{max(cAMP)}/I_{max(cGMP)}$ ratios from Table 1. For clarity, only the mean of all data points for each nucleotide concentration (± SE) is shown. Parameters that give the best fits and the number of experiments for each channel composition are listed in Table 1. Hill fits of cGMP and cAMP dose-response curves for *αwt* channels (*a*) are shown for comparison (·····) in *b*, *c*, *d*, and *e*.

of the 29 records (18–77 s, total length 1302 s) from the eight patches. The number of channels in the patch was measured at the end of the experiment (Fig. 3 *c)* by the addition of *N*-ethylmaleimide (2 mM) (Serre et al., 1995; Gordon et al., 1997), which increases $P_{0max(cGMP)}$ to almost 1; only single-channel records were retained. $P_{0max(cGMP)}$ in the presence of NEM was estimated to be 0.92 ± 0.03 from single-channel analysis. This allows a third independent determination of $P_{0max(cGMP)}$ from the ratio of macroscopic currents in the absence and in the presence of NEM: a value of 0.39 ± 0.02 (seven patches) was obtained for $I_{max(cGMP)}/I_{max(cGMP+NEM)}$, corresponding to a $P_{0max(cGMP)}$ of 0.36, close to the estimate obtained from Ni^{2+} potentiation. Thus, although there is a large variation between the different estimates (which is probably due to the fact that the estimate from single-channel analysis includes the low initial values, whereas estimates from macroscopic currents are obtained after stabilization of the currents), the $P_{0max(cGMP)}$ of *α*D604N channels is higher than reported by Sunderman and Zagotta (1999), whatever the method used.

In conclusion, coexpression of the *βwt* subunit with the *αwt* subunit reduces the gating efficacy of cGMP and increases that of cAMP. Similar though larger effects are produced by the D604N mutation in the *α* subunit.

Potentiation of cGMP-induced currents by low concentration of cAMP for homomeric (*αwt*) and heteromeric (*αwt*/*βwt* and *αwt*/*β*N1201D) channels

It was previously reported that in the native channel, low concentrations of cAMP, which alone induce a very low current, are able to potentiate cGMP-induced currents (Furman and Tanaka, 1989; Ildefonse et al., 1992). The effect is best observed for cGMP concentrations below EC_{50}. This effect was interpreted as an indication that the dissociation constant for cAMP is much lower than the EC_{50} measured from dose-response curves, which also depends on the capacity of the cAMP-bound channel to open. The question arises whether this phenomenon is also observed with expressed *α* channels. The fact that the *β* subunit increases the sensitivity to cAMP suggests that the potentiation by cAMP could be due to binding of cAMP with higher affinity to the *β* subunit than to the *α* subunit, which perhaps is due, at least in part, to N1201.

We have studied the potentiation of cGMP-induced currents by a low concentration of cAMP for three different channel compositions: *αwt*, *αwt*/*βwt*, and *αwt*/*β*N201D. Dose-response curves were measured on the same patch in the presence or absence of 100 *μ*M cAMP (which alone produces a very low current; see legend to Table 3). As an increase in apparent affinity for the nucleotide has been reported to spontaneously occur with time (Gordon et al., 1992; Molokanova et al., 1997), the current was measured three times for each cGMP concentration: first without cAMP, then with cAMP, and again without cAMP, to check the reversibility of the change. The curve obtained in the presence of cAMP and the average curve in the absence of cAMP were fitted to the Hill equation; the variations in EC_{50} (ΔEC_{50}) and n_H (Δn_H) were calculated for each experiment. The mean values of ΔEC_{50} and Δn_H from all experiments are listed in Table 3.

Fig. 4 shows mean data points from all experiments, normalized to the current at saturating cGMP concentration for each dose-response curve; the fits to the Hill equation shown on the graph were calculated with all data points. ΔEC_{50} and Δn_H for each channel composition are very similar to those obtained from the mean parameters of individual fits (Table 3).

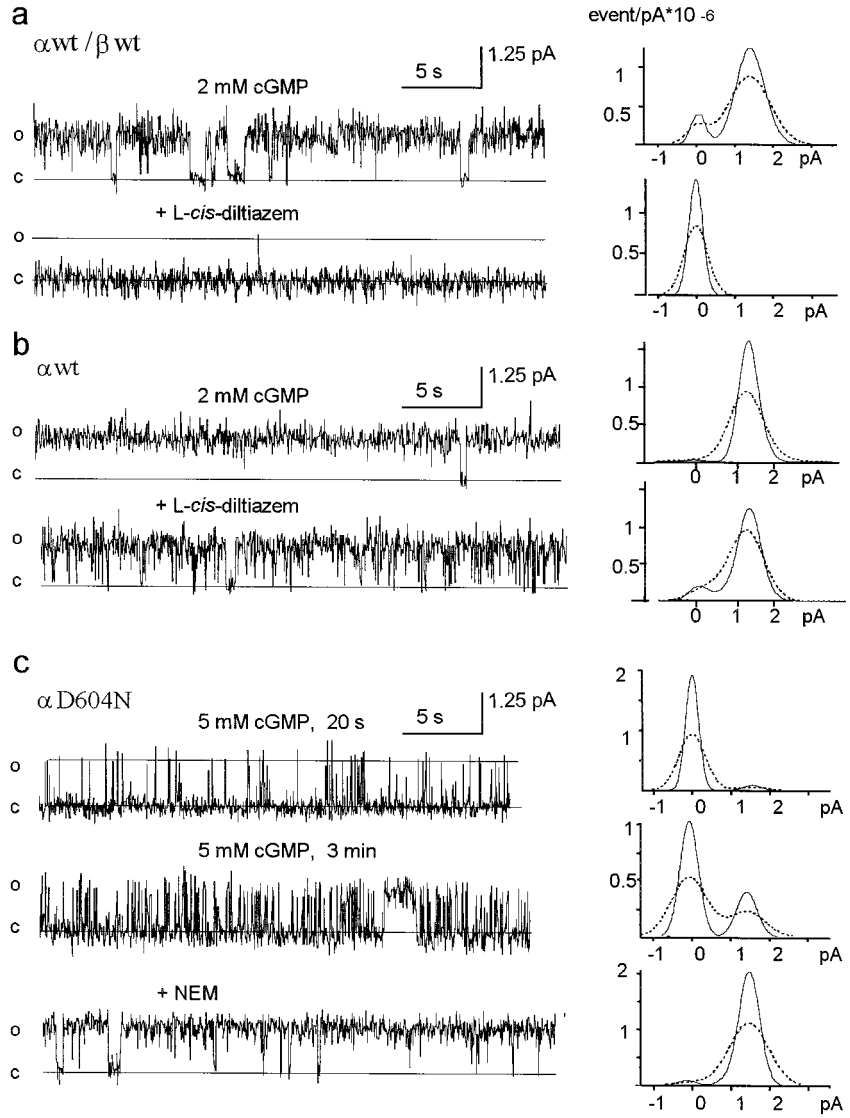

FIGURE 3 Single-channel records of expressed $\alpha wt/\beta wt$ (*a*), αwt (*b*), and αD604N (*c*) channels. Single-channel recording and analysis were performed as described in Materials and Methods. The records were filtered at 1 kHz for the figure. Amplitude histograms corresponding to the full records filtered at 4 kHz (·····) or 1 kHz (——) are shown. Histograms at 4 kHz were used to calculate P_{0max}. Values of P_{0max} for the examples shown are 0.88 and $\leq$0.01 ($\alpha wt/\beta wt$ in the absence or presence of 50 μM L-*cis*-diltiazem); 0.98 and 0.86 (αwt in the absence or presence of 50 μM L-*cis*-diltiazem); and 0.06 and 0.27 (αD604N after 20 s and 3 min in the presence of cGMP). For αD604N, NEM (2 mM) was added to the bath at the end of the experiment to check the number of channels in the patch (a single channel in the example shown).

Table 3 and Fig. 4 show that potentiation by cAMP is not observed for homomeric αwt channels. The presence of cAMP may even slightly inhibit the cGMP-induced current: for each of the eight experiments, the EC_{50} of the dose-response curve for cGMP in the presence of 100 μM cAMP was slightly increased compared to that in the absence of cAMP. Potentiation by cAMP (reduction of EC_{50} for cGMP), however, is observed for the two heterooligomeric

TABLE 2 Estimates of the open probability for different subunit compositions

	$P_{0max(cGMP)}$		$^*P_{0max(cAMP)}$	
mRNA injected	$I_{max(cGMP)}/I_{max(cGMP+Ni)}$	Single channel	$I_{max(cAMP)}/I_{max(cGMP+Ni)}$	Single channel
αwt	0.97 ± 0.01 (8)	0.96 ± 0.01 (8)	0.035 ± 0.01	0.034 ± 0.01
$\alpha wt + \beta wt$	0.88 ± 0.01 (15)	0.85 ± 0.03 (9)	0.13 ± 0.02	0.13 ± 0.02
αD604N	0.35 ± 0.04 (17)	0.25 ± 0.04 (8)	0.21 ± 0.04	0.15 ± 0.03

$P_{0max(cGMP)}$ was estimated by Ni^{2+} potentiation and single-channel analysis, as described in Materials and Methods. The number of experiments is indicated in parentheses. Mean values are given ± SE.

$^*P_{0max(cAMP)}$ was calculated from the values of $P_{0max(cGMP)}$ and the $I_{max(cAMP)}/I_{max(cGMP)}$ ratios given in Table 1; the error in $P_{0max(cAMP)}$ is the sum of relative errors in $P_{0max(cGMP)}$ and $I_{max(cAMP)}/I_{max(cGMp)}$, multiplied by the value of $P_{0max(cAMP)}$.

From independent *t*-tests of two populations, $I_{max(cGMP)}/I_{max(cGMP+Ni)}$ for αwt and $\alpha wt + \beta wt$ channels are significantly different with $p < 10^{-6}$. $P_{0max(cGMP)}$ for αwt and $\alpha wt + \beta wt$ from single-channel analysis are significantly different with $p < 0.003$.

TABLE 3 Difference between Hill parameters of cGMP dose-response curves measured in the absence and in the presence of 100 μM cAMP

mRNA injected	ΔEC_{50} (μM)	Δn_H
αwt	$+1.1 \pm 0.5$ (8)	-0.14 ± 0.04 (8)
$\alpha wt + \beta wt$	-10.8 ± 0.2 (11)	-0.34 ± 0.1 (10)
$\alpha wt + \beta$N1201D	-3.1 ± 0.3 (9)	-0.18 ± 0.03 (9)

Complete dose-response curves for cGMP were measured on the same patch in the presence or absence of 100 μM cAMP; for each cGMP concentration, the current was first measured in the absence of cAMP, then in the presence of cAMP, and again in the absence of cAMP. The differences between the values of EC_{50} ($\Delta EC_{50} = EC_{50(cGMP)} - EC_{50(cGMP+cAMP)}$) and n_H ($\Delta n_H = n_{H(cGMP)} - n_{H(cGMP+cAMP)}$) obtained by fitting the data in the presence or absence of cAMP to the Hill equation were calculated for each patch (the two points measured in the absence of cAMP were averaged for the fit). The mean values indicated in the table are the means of the differences obtained for each patch, $\pm$ SE. The number of experiments is indicated in parentheses. From independent *t*-tests of the two populations of EC_{50} (obtained from the fits of each experiment in the presence and in the absence of cAMP), the data in the presence or absence of cAMP for αwt channels are not significantly different, although for each individual experiment, the EC_{50} in the presence of cAMP was reproducibly higher than that in the absence of cAMP. Data for $\alpha wt/\beta wt$ channels in the presence and absence of cAMP are significantly different with $p = 4 \times 10^{-4}$, and data for $\alpha wt/\beta$N1201D channels are significantly different with $p = 0.03$. The ratio of the current induced by 100 μM cAMP in the absence of cGMP to $I_{max(cGMP)}$ was 0.003 ± 0.001 for αwt (eight experiments) and $\alpha wt + \beta wt$ (12 experiments) and 0.004 ± 0.001 for $\alpha wt + \beta$N1201D (nine experiments). Fig. 4 shows the fit of all data points from all experiments in the presence or absence of cAMP (normalized to the current at saturating cGMP concentration) together with the mean value ($\pm$ SE) of all of the data points at each cGMP concentration.

channels, but the effect is clearly more pronounced for βwt than for βN1201D.

DISCUSSION

Comparison between the functional properties of homomeric αwt channels, heteromeric channels from coexpressed αwt and βwt subunits, and native channels

While this work was in progress, Shammat and Gordon (1999) published a study of the coexpression of the wild-type bovine rod α subunit and human rod β subunit, in which they compare the $I_{max(cAMP)}/I_{max(cGMP)}$ ratio for the two channel types. Our results with coexpressed wild-type bovine α and β subunits are totally consistent with their results: the value of the $I_{max(cAMP)}/I_{max(cGMP)}$ ratio (15%, Fig. 1, compared to 13% in Shammat and Gordon, 1999) is significantly higher than for homomeric α channels and comparable to that previously obtained from native channels (Tanaka et al., 1989; Gavazzo et al., 1996; Picco et al., 1996). Although Scott and Tanaka (1998) report that coexpression of the β subunit with the α subunit does not restore the native $I_{max(cAMP)}/I_{max(cGMP)}$ ratio, it should be noted that, as shown in Fig. 1, the effect may be unnoticed if currents are measured at negative voltage, because of the very low amplitude of the currents.

Similar EC_{50} values for cGMP for homomeric α and heteromeric α/β channels were previously reported by Chen et al. (1993) (60–80 μM at +60 mV, human rod), Körshen et al. (1995) (40 μM at +80 mV, bovine rod), Scott and Tanaka (1998) (80 μM), and Shammat and Gordon (1999) (77 ± 31 μM and 63 ± 30 μM at +100 mV), although there is some variation in the value itself. Altenhofen et al. (1991) report a value for expressed bovine α subunits (32 ± 13 μM at +80 mV) that is closer to our value.

The value of the open probability obtained for αwt channels ($P_{0max(cGMP)} = 0.97$ from Ni^{2+} potentiation, or 0.96 from single-channel analysis; Table 2) is consistent with previous reports: $P_{0max} = 0.9$ from noise analysis (Goulding et al., 1994); 0.78 from single-channel measurements (Bucossi et al., 1997); 0.96 ± 0.01 from the ratio of $I_{max(cGMP)}$ in the presence or absence of Ni^{2+}; or 0.95 from single-channel recordings (Sunderman and Zagotta, 1999). No report concerning the open probability of expressed heteromeric α/β channels is as yet available. Torre et al. (1997) published a single-channel study of coexpressed bovine α and β subunits, where they describe three channel types with different properties, but they do not give any estimate of P_{0max}. Our estimates of $P_{0max(cGMP)}$ for $\alpha wt/\beta wt$ channels from single-channel analysis (0.85 ± 0.03, +80 mV) and Ni^{2+} potentiation (0.88 ± 0.01, +80 mV) are higher than previous measurements on native rods; from a single-channel kinetic analysis Taylor and Baylor (1995) obtained values of $P_{0max} = 0.56$ (+50 mV) and 0.30 (−50 mV), consistent with the report of Matthews and Watanabe (1988) (0.30 ± 0.05 at −71 mV). These works, however, were both performed on amphibian rods, with Na^+ as the permeating cation. Our results suggest that Ni^{2+} potentiation is a reliable method for estimating the open probability of heteromeric α/β channels, as previously demonstrated for homomeric α channels by Sunderman and Zagotta (1999).

Because α subunits alone can form functional channels and β subunits alone cannot, a mixed population of homomeric α and mixed heteromeric α/β channels ($\alpha_2\beta_2$ and $\alpha_3\beta$) could be expected when α and β subunits are coexpressed (as well as for native channels). (With a β:α mRNA ratio = 2 (3), assuming that the two messengers are translated with the same efficiency, that the stabilities of the two proteins are equivalent, and that channels with three or four β subunits are not functional, the probabilities of forming homomeric α, heteromeric $\alpha_3\beta$, and heteromeric $\alpha_2\beta_2$ would be, respectively, 3 (1.5)%, 24 (18)%, and 73 (80)%.) In this case, the values measured from macroscopic currents for $I_{max(cAMP)}/I_{max(cGMP)}$ and $P_{0max(cGMP)}$ would be intermediate between those for α/β channels and those for α channels. The results of Shammat and Gordon (1999), however, suggest that when α and β mRNAs are coinjected, even at a 1:1 ratio, only heteromeric $\alpha_2\beta_2$ channels are

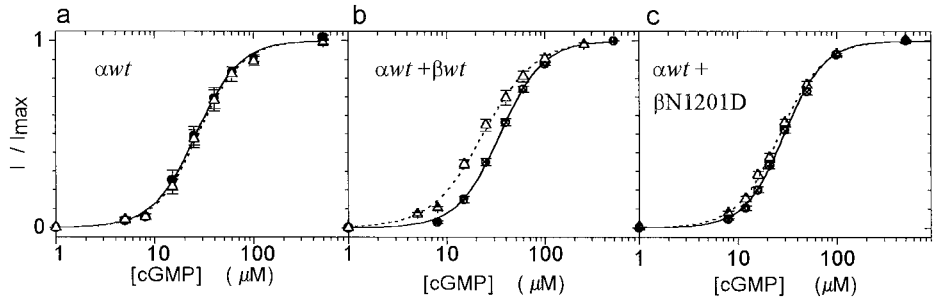

FIGURE 4 cAMP-potentiation of cGMP-induced currents in oocytes injected with mRNAs for αwt (*a*), *αwt* + *βwt* (*b*), and *αwt* + βN1201D (*c*). ●, In the absence of cAMP; △, in the presence of 100 μM cAMP. Currents induced by each cGMP concentration were measured first in the absence of cAMP, then in the presence of 100 μM cAMP, and again in the absence of cAMP (*a:* eight experiments; *b:* 11 experiments; *c:* nine experiments). The currents induced by cGMP or by cGMP + cAMP were normalized to the value at saturating cGMP concentration. No increase in the current at saturating cGMP concentration was observed in the presence of added cAMP. The curves are the best fits of all of the normalized data to the Hill equation: *a* (*αwt*): EC_{50} = 26.3 ± 1 μM, n_H = 2 ± 0.14 (without cAMP, ——), EC_{50} = 27.6 ± 1 μM, n_H = 1.95 ± 0.1 (with cAMP, – – –); *b* (*αwt*/*βwt*): EC_{50} = 35 ± 0.6 μM, n_H = 2 ± 0.1 (without cAMP, ——), EC_{50} = 24 ± 0.7 μM, n_H = 1.65 ± 0.1 (with cAMP, – – –); *c* (*αwt*/βN1201D): EC_{50} = 29.9 ± 0.4 μM, n_H = 2.15 ± 0.06 (without cAMP, ——), EC_{50} = 26.8 ± 0.4 μM, n_H = 1.97 ± 0.06 (with cAMP, – – –). For clarity, only the mean values of data points obtained for each cGMP concentration from all experiments are indicated (± SE). The data in the presence or absence of cAMP for each experiment were also fit individually to the Hill equation (not shown); mean values of the variation in EC_{50} and in n_H obtained for each experiment are listed in Table 3.

formed. Our single-channel records of patches from oocytes coinjected with α and β mRNA in the presence of L-*cis*-diltiazem suggest that, for an α:β mRNA ratio of 3, only a few homomeric α channels may coexist with heteromeric channels.

Our results agree with those of Scott and Tanaka (1998) concerning the restoration of potentiation of cGMP-induced currents by low concentrations of cAMP by coexpression of the β subunit; the potentiation by cAMP of cGMP-induced currents observed with coexpressed α and β subunits is similar to that previously described for native channels (Furman and Tanaka, 1989; Ildefonse et al., 1992). Because evolution of the channel characteristics has been reported to occur spontaneously with time (Gordon et al., 1992; Molokanova et al., 1997), seemingly because of dephosphorylation of the channel, we have been very careful to check that the effect of cAMP on the cGMP-induced currents is reversible. Moreover, it should be noted that in our potentiation experiments, preliminary control measurements (leak current, current induced by 100 μM cAMP, current at saturation of cGMP and cAMP) are performed before measurements for dose-response curves and take several minutes (usually more than 5 min). The decrease in EC_{50} for α channels expressed in oocytes described by Molokanova et al. (1997) is a fast process, which becomes negligible ~5 min after patch excision.

Role of the charge of residue 604 in the α subunit and 1201 in the β subunit in the sensitivity to cAMP, cAMP potentiation of cGMP-induced currents, and gating efficacy of cGMP

We have studied the role of the charge of residue 604/1201 in three aspects of channel function: sensitivity to cAMP (EC_{50} and $I_{max(cAMP)}/I_{max(cGMP)}$ ratio), gating efficacy of cGMP ($P_{0max(cGMP)}$), and cAMP potentiation of cGMP-induced currents.

The results show that, as previously reported (Varnum et al., 1995), replacing D604 in the α subunit by the uncharged residue N, which is present at the corresponding place in the β subunit, increases the $I_{max(cAMP)}/I_{max(cGMP)}$ ratio. We also show that coexpressing the *βwt* subunit with the *αwt* subunit produces qualitatively similar (but smaller) effects, as is expected if the effect is due to the presence of an uncharged residue in position 604/1201, because the heteromeric channel has both D and N in position 604/1201, instead of 4N in αD604N. However, coexpressing the *βwt* subunit with αD604N further increases the sensitivity to cAMP ($I_{max(cAMP)}/I_{max(cGMP)}$ ratio and EC_{50}), and replacing N1201 by D in the β subunit does not restore the characteristics of the α homooligomer: *αwt*/βN1201D, which has 4 D in positions 604/1201, is intermediate between wild-type *αwt*/*βwt* (in which both D and N are present) and α channels (which also have 4 D in position 604).

Similarly, although βN1201D is less efficient than *βwt*, significant potentiation by cAMP of cGMP-induced currents is observed when the mutated β subunit is coexpressed with the α subunit.

Another effect of the D604N mutation is to reduce the channels' open probability for cGMP compared to *αwt* channels ($P_{0max(cGMP)}$ = 0.35 from Ni^{2+} potentiation or 0.25 from single-channel analysis; Table 2). These values are much higher than those reported by Sunderman and Zagotta (1999) with the same methods; as noted in the Results, the discrepancy could be due to the combined effect of the nature of the permeating cation, and the slow response of αD604N channels to cGMP, the low values (0.07–0.08) measured by Sunderman and Zagotta (1999)

being closer to the values that we usually obtain during the first minute in the presence of cGMP (Fig. 3 *c*). The $P_{0max(cGMP)}$ value measured for αD604N channels by Varnum et al. (1995) also seems higher than that reported by Sunderman and Zagotta (1999) (see below). The reduction of the gating efficacy of cGMP is also observed, although less marked, with the coexpression of the *αwt* and *βwt* subunits ($P_{0max(cGMP)}$ = 0.88 or 0.85, according to the method used).

It can therefore be concluded that the charge of residue 604/1201 plays an important role in the sensitivity to cAMP, the gating efficacy for cGMP, and cAMP potentiation of cGMP-induced currents; however, other part(s) of the proteins participate in these effects. In addition, only a moderate (if significant) increase in the EC_{50} for cGMP is observed when *αwt* and *βwt* are coexpressed, whereas a 15-fold increase is observed with αD604N channels, also suggesting a role of other parts of the protein in the sensitivity to cGMP. It can be proposed that other residues in the binding site or in another domain (for example, in the C-linker; Zong et al., 1998; Paoletti et al., 1999) are determinants of the action of the nucleotide.

Interpretation of the data in terms of affinity and gating efficacy of the ligand

The open probability at the saturating concentration of nucleotide, i.e., when all of the binding sites are occupied (P_{0max}), is an indication of the gating efficacy of the nucleotide. Independently of the model, as long as unliganded (or partially liganded) channel openings are negligible compared to fully liganded channel openings, the constant for the gating transition,

$$\underset{\text{(closed)}}{C(cNMP)_4} \underset{K_{op}}{\rightleftharpoons} \underset{\text{(open)}}{O(cNMP)_4}$$

can be calculated from the experimental estimates of P_{0max}:

$$K_{op} = [\text{open channels}]/[\text{closed channels}]$$
$$= P_{0max}/(1 - P_{0max}).$$

Using the estimates of P_{0max} from Table 2 for the three channel types (*αwt*, αD604N, and *αwt*/*βwt*), we calculate that the free energies of gating ($\Delta G_{op} = -RT \ln[K_{op}]$) upon coexpression of the β subunit with the α subunit are intermediate between those for *αwt* channels and those for αD604N channels. The decrease in the free energy of gating by cAMP for D604N channels compared to *αwt* (Table 5) is larger than (but less than twice) that for *αwt*/*βwt* channels, and the increase in the free energy of gating by cGMP for αD604N channels compared to the *αwt* channel is more than twice that for the heteromeric channel compared to the *αwt* channel. If the effect on gating was only due to the charge of residue 604/1201, and if the α and β subunits assemble as an ααββ oligomer, as proposed by Shammat and Gordon (1999), a factor of 2 would be expected between $\Delta\Delta G_{op}$ for αD604N and *αwt*/*βwt* channels compared to *αwt*. Our results may indicate that improved gating by cAMP upon coassembly of the β subunit is not due solely to residue N1201 (consistent with the conclusions drawn from the $I_{max(cAMP)}/I_{max(cGMP)}$ ratios measured for heteromeric *αwt*/βN1201D and αD604N/*βwt* channels), and that reduced gating by cGMP of α D604N involves residues other than N604. Our results with αD604N channels are consistent with those of Varnum et al. (1995), who calculated that the free energy of gating for cAMP was reduced by ~1.3 kcal/mol by mutations of D604 to neutral residues, whereas that for cGMP was increased by 2 kcal/mol for D604N. This indicates that the $P_{0max(cGMP)}$ measured by these authors for αD604N channels in this work is closer to our estimate (0.30 ± 0.05) than to the estimate given by Sunderman and Zagotta (1999) (0.07–0.08), which would produce a much larger $\Delta\Delta G$.

Using a simplified linear scheme with two binding sites, Varnum et al. (1995) find that the free energy of initial binding is not substantially altered by mutations at position 604. They conclude that interaction of the purine ring of the nucleotide with D604 in the αC helix is important for the conformational change leading to channel opening rather than for initial binding. However, the value of the binding constant depends on the model chosen to calculate it. Although the linear model has proved useful in interpreting the effects of mutations in the α subunit (Gordon and Zagotta, 1995; Varnum et al., 1995), a fundamental aspect of CNG channel function is the existence of spontaneous openings in the absence of ligand (Picones and Korenbrot, 1995; Goulding et al., 1994; Tibbs et al., 1997; Ruiz and Karpen, 1997), which is not compatible with simple linear models of activation, in which channels can only open after binding of the ligand. Several allosteric models, including the Monod-Wyman-Changeux (MWC) concerted model (Monod et al., 1965; used by Goulding et al., 1994; Varnum and Zagotta, 1996; Tibbs et al., 1997; Paoletti et al., 1999), a coupled-dimer model in which two independent dimers undergo a concerted allosteric transition (Liu et al., 1998), and a complete scheme including intermediate states (Ruiz and Karpen, 1999) have been recently shown to be better adapted for the description of CNG channel function. In the case of heteromeric channels, the models should in fact be modified to include different characteristics for the two types of subunits, but this would increase the number of parameters and increase the uncertainty in the fitting operation. We have therefore used the simple MWC model to fit the results, as an approximation that should be closer to the real mechanism of activation than the linear model used by Varnum et al. (1995), to obtain the binding constants for the nucleotide. Fitting the data with the coupled dimer model

(Liu et al., 1998) gives qualitatively similar results (not shown).

In the MWC and derived models, the protein can exist in two states (T, corresponding to the closed state, and R, corresponding to the open state of the channel); the T state has a lower affinity than the R state for the ligand ($c = K_R/K_T \ll 1$, where K_R and K_T are the dissociation constants for the open and closed states). The transition between T and R is disfavored in the absence of ligand ($L = [T]/[R] \gg 1$) and is increasingly favored upon ligand binding because of the higher affinity for the R state. The MWC model for a tetramer is represented by the following scheme (see also Materials and Methods):

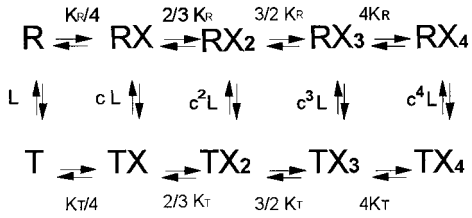

The $\bar{R}$ function represents the proportion of channels in the R (open) state, and its variation as a function of ligand concentration simulates the variation of the open probability. For clarity, we will use below the parameter c for cGMP ($c = K_{RG}/K_{TG}$, where K_{RG} and K_{TG} are the dissociation constants of the open and closed states for cGMP) and the parameter d for cAMP ($d = K_{RA}/K_{TA}$, where K_{RA} and K_{TA} are the dissociation constants of the open and closed states for cAMP).

Comparison of data obtained with αwt and data obtained with $\alpha wt/\beta wt$ or with αD604N, which show a lower P_{0max} for cGMP and a higher $I_{max(cAMP)}/I_{max(cGMP)}$ for the $\alpha wt/\beta wt$ heterooligomer and for αD604N than for αwt, suggests that the difference is not due to a modification of L, which should produce similar modifications for the two ligands (see Materials and Methods), but rather to modifications of c and d, although it cannot be excluded that L is also modified, but that the modification due to L is masked by larger modifications due to c and d. This was also proposed by Varnum and Zagotta (1996) for mutations of D604 in the α subunit from interpretation of their data with the MWC model. We have therefore searched for values of K_{RG} and c (cGMP), K_{RA} and d (cAMP) that are consistent with the data for a fixed value of L ($L = 7999$, calculated from the value for spontaneous open probability $P_{sp} = 1.25 \times 10^{-4}$ reported by Tibbs et al. (1997)). The experimental data that were used in Fig. 2 for three channel types (αwt, $\alpha wt/\beta wt$, and αD604N), corrected for the P_{0max} values indicated in Table 2, were fitted to the $\bar{R}$ function of the MWC model. As in Fig. 2, fits were performed using all of the data points from all experiments. Fig. 5 only shows the fits corresponding to the P_{0max} values obtained from single-channel analysis for the three channel types. Parameters that give the best fit of the data for both estimates of the $P_{0max(cGMP)}$ are indicated in Table 4.

Dose-response curves measured upon coexpression of βwt with αwt are fitted with reduced K_{RA} and K_{TA}, compared to the values that fit dose-response curves of αwt, the effect being more marked for K_{RA}, which corresponds to a decrease in d (increasing the gating efficacy of cAMP); coexpression of βwt with αwt, which reduces the gating efficacy of cGMP (Table 2), also results in increasing c and consequently increased selectivity for cAMP versus cGMP. The difference between parameters obtained for the $\alpha wt/\beta wt$ heteromeric channel and for the αwt homomeric channel can be interpreted in two ways: 1) the parameters

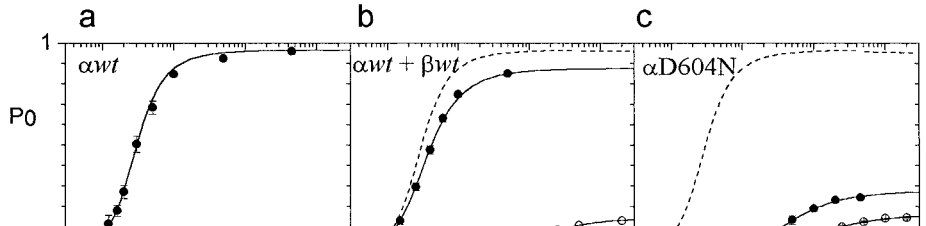

FIGURE 5 Fits of dose-response curves according to the MWC model (Monod et al., 1965) for αwt (*a*), $\alpha wt/\beta wt$ (*b*), and αD604N (*c*) channels. ●, cGMP; ○, cAMP. Normalized data points from all experiments used for the dose-response curves shown in Fig. 2 were fitted to the $\bar{R}$ function of the MWC model (see Materials and Methods), after the currents were corrected at saturating nucleotide concentrations for the P_{0max} values from Table 2. The data in the figure were corrected for the $P_{0max(cGMP)}$ estimated from single-channel analysis. For clarity, only the mean values of all data points obtained for each ligand concentration are shown in the figure (± SE). A fixed value of L, calculated from the value of spontaneous channel openings $P_{sp} = 1.25 \times 10^{-4}$ measured by Tibbs et al. (1997), was used: $L = 1/P_{sp} - 1 = 7999$. The free parameters were K_{RG} and c (cGMP), K_{RA} and d (cAMP). Fits for αwt channels (from *a*) are indicated in *b* and *c* (– – –). Parameters that give the best fit are given in Table 4. Note that the slopes of the different dose-response curves (reduced n_H for cAMP compared to cGMP for αwt-containing channels, and reduced n_H for cGMP for αD604N compared to αwt channels, Table 1) are well simulated by the MWC model, in which an increase in the parameter c (which reflects the gating efficacy of the ligand) results in a reduction of the Hill number (Rubin and Changeux, 1966).

TABLE 4 MWC parameters of the fits of Fig. 5

		cGMP			cAMP		
mRNA injected	$P_{0max(cGMP)}$	c	K_{RG} (μM)	K_{TG} (μM)	d	K_{RA} (μM)	K_{TA} (μM)
αwt	0.97	0.052 ± 0.002	1.89 ± 0.08	36 ± 3	0.242 ± 0.003	149 ± 18	616 ± 82
	*0.96	0.046 ± 0.003	2.01 ± 0.09	43 ± 5	0.238 ± 0.003	146 ± 18	613 ± 83
$\alpha wt + \beta wt$	0.88	0.061 ± 0.001	1.93 ± 0.03	32 ± 1	0.166 ± 0.001	79 ± 0.4	477 ± 3
	*0.85	0.065 ± 0.001	1.89 ± 0.04	29 ± 1	0.166 ± 0.001	79 ± 0.4	477 ± 3
αD604N	0.35	0.119 ± 0.002	20 ± 1.6	168 ± 16	0.146 ± 0.001	63 ± 4	431 ± 30
	*0.25	0.135 ± 0.001	20.8 ± 1.2	154 ± 10	0.161 ± 0.001	68 ± 4.5	422 ± 30

L is calculated from the value of spontaneous channel openings, $P_{sp} = 1.25 \times 10^{-4}$, measured by Tibbs et al. (1997) ($L = 7999$). Taking a value for spontaneous openings of 10^{-5} (similar to that measured by Goulding et al. (1994) and by Ruiz and Karpen (1997), which gives a value of $L = 10^5$, does not qualitatively change the results (not shown); the values of all parameters are decreased by a factor close to 2 compared to the values indicated in the table. The errors in the values of the parameters are calculated with Origin software (see Materials and Methods). The values of K_{TG} and K_{TA} listed in the table were calculated from the values of K_{RG} and c, K_{TA} and d, obtained from the fit of the data. Two fits are indicated for each channel type, corresponding to the estimates for the open probability in the presence of cGMP (from Table 2). Only the fits corresponding to the P_0 estimated from single-channel analysis (indicated by *) are shown in Fig. 5.

obtained for heteromeric channels are intermediate between those for αwt and those for βwt subunits, which differ because of the distinct intrinsic properties of the two subunits; or 2) coexpression of the β subunit with the α subunit modifies the behavior of the α subunit, as proposed by Karpen and Brown (1996). According to the former hypothesis, cAMP would have a better affinity and better gating efficacy for β subunits than for α subunits, while cGMP would have a similar affinity for the two subunits and a reduced gating efficacy for β subunits. According to the latter hypothesis, it is not possible to discriminate between the properties of the two types of subunits, and the α/β oligomer should be considered as a global entity. However, if the channel is composed of an α dimer and a β dimer with dimerization of the cyclic nucleotide binding sites, as proposed by Shammat and Gordon (1999) and by Liu et al. (1998), the existence of interactions between α and β subunits at the level of the binding sites appears unlikely.

The effect of the D604N mutation in the α homomeric channel compared to the wild-type channel, from Table 4, is to reduce the affinity of both states for cGMP and to increase the affinity (mainly of the open state) for cAMP, which corresponds to an increase in c and a decrease in d. Thus the D604N mutation mimics the effect of coexpression of the β subunit on the selectivity for cAMP, supporting the hypothesis that β subunits have an increased affinity and gating efficacy for cAMP compared to α subunits, even though, as discussed above, the charge of residue 604/1201 cannot solely account for the different sensitivities of the homo- and heterooligomers for cAMP. The effect of the D604N mutation on the affinities of the two states for cGMP, however, is much more dramatic than that of subunit coassembly. Note that fitting the data obtained for αwt, $\alpha wt/\beta wt$, and αD604N channels for the two estimates of $P_{0max(cGMP)}$ (from Table 2) leads to qualitatively similar conclusions (Table 4); in particular, the values of the dissociation constants are little modified, even for αD604N channels for which the two P_{0max} estimates are the most divergent.

The variations in the free energy of nucleotide binding (open and closed states) for heteromeric $\alpha wt/\beta wt$ channels or αD604N channels compared to αwt channels, calculated according to the MWC model from the values in Table 4, are given in Table 5. For both $\alpha wt/\beta wt$ and αD604N channels compared to αwt channels, the variation in free energy of cAMP binding to the closed and open states is low

TABLE 5 Variation of the free energy of gating and binding upon coassembly of αwt and βwt subunits and upon mutating D604 in the α subunit by comparison with αwt channels

	$\Delta\Delta G$ (kcal/mol) = ΔG(channel) − $\Delta G(\alpha wt)$					
	cGMP			cAMP		
Channel	$\Delta\Delta G_{op}$	$\Delta\Delta G^{R}_{bind}$	$\Delta\Delta G^{T}_{bind}$	$\Delta\Delta G_{op}$	$\Delta\Delta G^{R}_{bind}$	$\Delta\Delta G^{T}_{bind}$
$\alpha wt/\beta wt$	+0.9 ± 0.5	0 ± 0.1	−0.1 ± 0.1	−0.85 ± 0.1	−0.35 ± 0.1	−0.1 ± 0.1
αD604N	+2.5 ± 0.6	+1.4 ± 0.1	+0.85 ± 0.1	−1.1 ± 0.3	−0.5 ± 0.2	−0.2 ± 0.15

The free energy of gating is $\Delta G_{op} = -RT\ln(K_{op})$, where $K_{op} = P_{0max}/(1 - P_{0max})$, and the free energy of nucleotide binding is $\Delta G_{bind} = -RT\ln(K_a)$, where K_a is the affinity ($= 1/K_d$) for the nucleotide (M^{-1}). ΔG^{R}_{bind} corresponds to binding to the open state (R) and ΔG^{T}_{bind} to the closed state (T). The variation in free energy of gating ($\Delta\Delta G_{op}$) or nucleotide binding ($\Delta\Delta G^{R}_{bind}$ and $\Delta\Delta G^{T}_{bind}$) upon coassembly of subunits or upon mutation of D604 compared to αwt channels is the difference between each ΔG and the corresponding ΔG for αwt. P_{0max} and dissociation constants (K_{RG}, K_{TG}, K_{RA}, K_{TA}) used for calculations are the means of the two estimates given in Tables 2 and 4, and the error is taken as the difference between the mean and each value plus the largest SE. $T = 22°C$.

compared to the variation in the free energy of gating by cAMP (see above and Table 5), as noted by Varnum et al. (1995) for αD604N channels with the linear model. On the other hand, there is a marked difference between αD604N and *αwt*/*βwt* channels concerning the free energy of cGMP binding: the shifts in the affinity for cGMP in the αD604N compared to the *αwt* channel are much larger than for *αwt*/*βwt*, and the corresponding $\Delta\Delta G$ ($\Delta\Delta G^{R}_{bind} \approx +1.4$ kcal/mol, $\Delta\Delta G^{T}_{bind} \sim +0.85$ kcal/mol) are much larger than those for the heteromeric *αwt*/*βwt* channel, which are close to 0. This suggests that other residues of the α subunit, either within the same subunit or from adjacent subunits, increase the negative effect of the uncharged residue in position 604 on cGMP binding (or that other residues in the β subunit decrease this effect). (A smaller $\Delta\Delta G_{binding}$ for αD604N channels compared to *αwt* channels was reported by Varnum et al. (1995), using the linear model with two binding sites to calculate the binding constants (~ +0.5 kcal/mol). With the same model and with the P_{0max} and EC_{50} from Tables 1 and 2, a similar value (+0.4 or +0.5 kcal/mol) is obtained for αD604N channels; for *αwt*/*βwt* channels, however, the variation in free energy of cGMP binding compared to *αwt* channels is negative (−0.4 or −0.3 kcal/mol), also suggesting that the charge of residue 604/1201 is not determinant for the sensitivity to cGMP.) Note, however, that these values are small compared to the free energy of a hydrogen bond (~3.5 kcal/mol) or even an ionic bond (~2 kcal/mol) .

CONCLUSIONS

Coexpression of the β subunit with the α subunit restores both the sensitivity of native channels to cAMP ($I_{max(cAMP)}/I_{max(cGMP)}$ ratio) and potentiation of cGMP-induced current by low concentrations of cAMP; it also reduces the gating efficacy of cGMP. Results with mutated channels (αD604N, αD604N/*βwt*, and *αwt*/βN1021D) show that the charges of the residues in position 604 of the α subunit and in position 1201 of the β subunit play an important role in nucleotide binding and gating efficacy, as well as cAMP potentiation, but are not solely responsible for the differences between homomeric and heteromeric channels. With the MWC model (Monod et al., 1965), the higher sensitivity for cAMP in the presence of β subunit can be simulated by a better affinity of cAMP for the β subunit (or for the α/β heterooligomer taken as global entity) than for the α subunit alone, together with an increased selectivity for cAMP versus cGMP (reduced gating efficacy of cGMP and increased gating efficacy of cAMP). The data suggest that the D604N mutation in the α subunit as well as coassembly of α and β subunits mainly alter the free energy of gating by cGMP and cAMP; the D604N mutation, but not subunit coassembly, also increases the free energy of binding of cGMP.

We thank Prof. U. B. Kaupp for the gift of the cDNA for the rod α subunit, Dr. W. Altenhofen for help in starting patch-clamp experiments, and F. Piccarreta for technical assistance.

FP was the recipient of a fellowship from the Association Française Retinitis Pigmentosa (AFRP).

REFERENCES

Altenhofen, W., J. Ludwig, E. Eismann, W. Kraus, W. Bönigk, and U. B. Kaupp. 1991. Control of ligand specificity in cyclic nucleotide-gated channels from rod photoreceptors and olfactory epithelium. *Proc. Natl. Acad. Sci. USA.* 88:9868–9872.

Biel, M., X. Zong, A. Ludwig, A. Sautter, and F. Hofmann. 1996. Molecular cloning and expression of a modulatory subunit of the cyclic nucleotide-gated cation channel. *J. Biol. Chem.* 271:6349–6355.

Bradley, J., J. Li, N. Davidson, H. Lester, and K. Zinn. 1994. Heteromeric olfactory cyclic nucleotide-gated channel: a subunit that confers increased sensitivity to cAMP. *Proc. Natl. Acad. Sci. USA.* 91: 8890–8894.

Bucossi, G., M. Nizzari, and V. Torre. 1997. Single-channel properties of ionic channels gated by cyclic nucleotides. *Biophys. J.* 72:1165–1181.

Chen, T.-Y., Y.-W. Peng, R. S. Dhallan, B. Ahamed, R. R. Reed, and K.-W. Yau. 1993. A new subunit of the cyclic nucleotide-gated cation channel in retinal rod. *Nature.* 362:764–767.

Fodor, A. A., and W. N. Zagotta. 1996. Subunit 2 alters ligand specificity of rod CNG channels. *Biophys. J.* 70:A368 (Abstr.).

Furman, R. E., and J. C. Tanaka. 1989. Photoreceptor channel activation: interaction between cAMP and cGMP. *Biochemistry.* 28:2785–2788.

Gavazzo, P., C. Picco, L. Maxia, and A. Menini. 1996. Properties of native and cloned cyclic nucleotide gated channels from bovine. *In* Neurobiology: Ionic Channels, Neurons and the Brain. V. Torre and F. Conti, editors. Plenum Press, New York. 75–83.

Gordon, S. E., D. L. Brautigan, and A. L. Zimmermann. 1992. Protein phosphatases modulate the apparent agonist affinity of the light-regulated ion channel in retinal rods. *Neuron.* 9:739–748.

Gordon, S. E., J. C. Oakley, M. D. Varnum, and W. N. Zagotta. 1996. Altered ligand specificity by protonation in the ligand binding domain of cyclic nucleotide-gated channels. *Biochemistry.* 35:3994–4001.

Gordon, S. E., M. D. Varnum, and W. N. Zagotta. 1997. Direct interaction between amino- and carboxy-terminal domains of cyclic nucleotide-gated channels. *Neuron.* 19:431–441.

Gordon, S. E., and W. N. Zagotta. 1995. A histidine residue associated with the gate of the cyclic nucleotide-activated channels in rod photoreceptors. *Neuron.* 14:177–183.

Goulding, E. H., G. R. Tibbs, and S. A. Siegelbaum. 1994. Molecular mechanism of cyclic nucleotide-gated channel activation. *Nature.* 372: 369–374.

Ildefonse, M., and N. Bennett. 1991. Single-channel study of the cGMP-dependent conductance of retinal rods from incorporation of native vesicles into planar lipid bilayers. *J. Membr. Biol.* 123:133–142.

Ildefonse, M., S. Crouzy, and N. Bennett. 1992. Gating of retinal rod cation channel by different nucleotides: comparative study of unitary currents. *J. Membr. Biol.* 130:91–104.

Karpen, J. W., and R. L. Brown. 1996. Covalent activation of retinal rod cGMP-gated channels reveals a functional heterogeneity in the ligand binding sites. *J. Gen. Physiol.* 107:169–181.

Kaupp, U. B., T. Niidome, T. Tanabe, S. Terada, W. Bönigk, W. Stühmer, N. Cook, K. Kangawa, H. Matsuo, T. Hirose, T. Miyata, and S. Numa. 1989. Primary structure and functional expression from complementary cDNA of the rod cGMP-gated channel. *Nature.* 342:762–766.

Körschen, H. G., M. Illing, R. Seifert, F. Sesti, A. Williams, S. Gotzes, C. Colville, F. Müller, A. Dose, M. Godde, L. Molday, U. B. Kaupp, and R. S. Molday. 1995. A 240 kDa protein represents the complete β subunit of the cGMP-gated channel from rod photoreceptor. *Neuron.* 15:627–636.

Kozak, M. 1984. Compilation and analysis of sequences upstream from the translational start site in eukaryotic mRNAs. *Nucleic Acids Res.* 12: 857–872.

Liman, E. R., and L. B. Buck. 1994. A second subunit of the olfactory cyclic nucleotide-gated channel confers high sensitivity to cAMP. *Neuron.* 13:611–621.

Liman, E. R., J. Tytgat, and P. Hess. 1992. Subunit stoichiometry of a mammalian K^+ channel determined by construction of multimeric cDNAs. *Neuron.* 9:861–871.

Liu, D. T., G. R. Tibbs, P. Paoletti, and S. A. Siegelbaum. 1998. Constraining ligand-binding site stoichiometry suggests that a cyclic-nucleotide gated channel is composed of two functional dimers. *Neuron.* 21:235–248.

Liu, D. T., G. R. Tibbs, and S. A. Siegelbaum. 1996. Subunit stoichiometry of cyclic nucleotide-gated channels and effects of subunit order on channel function. *Neuron.* 16:983–990.

Matthews, G., and S.-I. Watanabe. 1988. Activation of single channels from toad retinal rod inner segments by cyclic GMP: concentration dependence. *J. Physiol. (Lond.).* 403:389–405.

Molokanova, E., B. Trivedi, A. Savchenko, and R. H. Kramer. 1997. Modulation of rod photoreceptor cyclic nucleotide-gated channels by tyrosine phosphorylation. *J. Neurosci.* 17:9068–9076.

Monod, J., J. Wyman, and J. P. Changeux. 1965. On the nature of allosteric transitions: a plausible model. *J. Mol. Biol.* 12:88–118.

Nizzari, M., F. Sesti, M. T. Giraudo, C. Virginio, A. Cattaneo, and V. Torre. 1993. Single channel properties of clones cGMP-activated channels from retinal rods. *Proc. R. Soc. Lond. B.* 254:69–74.

Paoletti, P., E. C. Young, and S. A. Siegelbaum. 1999. C-linker of cyclic nucleotide-gated channels controls coupling of ligand binding to channel gating. *J. Gen. Physiol.* 113:17–33.

Picco, C., C. Sanfilippo, P. Gavazzo, and A. Menini. 1996. Modulation by internal protons of native cyclic nucleotide-gated channels from retinal rods. *J. Gen. Physiol.* 108:265–276.

Picones, A., and J. I. Korenbrot. 1995. Spontaneous, ligand-independent activity of the cGMP-gated ion channels in cone photoreceptors of fish. *J. Physiol. (Lond.).* 485:699–714.

Rubin, M. M., and J. P. Changeux. 1966. On the nature of the allosteric transition: implications of non-exclusive ligand binding. *J. Mol. Biol.* 21:265–274.

Ruiz, M. L., and J. W. Karpen. 1997. Single cyclic nucleotide-gated channels locked in different ligand-bound states. *Nature.* 389:389–392.

Ruiz, M. L., and J. W. Karpen. 1999. Opening mechanism of a cyclic nucleotide-gated channel based on analysis of single channels locked in each liganded state. *J. Gen. Physiol.* 113:873–895.

Sautter, A., X. Zong, F. Hofmann, and M. Biel. 1998. An isoform of the rod photoreceptor cyclic nucleotide-gated channel β subunit expressed in olfactory neurons. *Proc. Natl. Acad. Sci. USA.* 95:4696–4701.

Scott, S.-P., and J. C. Tanaka. 1998. The β subunit of the cyclic nucleotide-gated channel (CNGC) confers native-like properties to the currents when co-transfected with the α subunit. *Biophys. J.* 74:A125 (Abstr.).

Serre, V., M. Ildefonse, and N. Bennett. 1995. Effects of cysteine modification on the activity of the cGMP-gated channel from retinal rods. *J. Membr. Biol.* 146:145–152.

Shabb, J. B., and J. D. Corbin. 1992. Cyclic nucleotide-binding domains in proteins having diverse functions. *J. Biol. Chem.* 267:5723–5726.

Shammat, I. M., and S. E. Gordon. 1999. Stoichiometry and arrangement of subunits in rod cyclic nucleotide-gated channels. *Neuron.* 23: 809–819.

Sunderman, E. R., and W. N. Zagotta. 1999. Sequence of events underlying the allosteric transition of rod cyclic nucleotide-gated channels. *J. Gen. Physiol.* 113:621–640.

Tanaka, J. C., J. F. Eccleston, and R. E. Furman. 1989. Photoreceptor channel activation by nucleotide derivatives. *Biochemistry.* 28: 2776–2784.

Taylor, W. R., and D. A. Baylor. 1995. Conductance and kinetics of single cGMP-activated channels in salamander rod outer segments. *J. Physiol. (Lond.).* 483:567–582.

Tibbs, G. R., E. H. Goulding, and S. A. Siegelbaum. 1997. Allosteric activation and tuning of ligand efficacy in cyclic nucleotide-gated channels. *Nature.* 386:612–615.

Torre, V., M. Straforini, F. Sesti, and T. D. Lamb. 1992. Different channel-gating properties of two classes of cyclic GMP-activated channels in vertebrate photoreceptors. *Proc. R. Soc. Lond. B.* 250:209–215.

Varnum, M. D., K. D. Black, and W. N. Zagotta. 1995. Molecular mechanism for ligand discrimination of cyclic nucleotide-gated channel. *Neuron.* 15:619–625.

Varnum, M. D., and W. N. Zagotta. 1996. Subunit interactions in the activation of cyclic nucleotide-gated ion channels. *Biophys. J.* 70: 2667–2679.

Zimmerman, A. L., J. W. Karpen, and D. A. Baylor. 1988. Hindered diffusion in excised membrane patches from retinal rod outer segments. *Biophys. J.* 54:351–355.

Zong, X., H. Zucker, F. Hofmann, and M. Biel. 1998. Three amino acids in the C-linker are major determinants of gating in cyclic nucleotide-gated channels. *EMBO J.* 17:353–362.